RESEARCH ARTICLE

Synthesis of Resin-based Composites Containing Cellulose Nanocrystal and Nano-amorphous Calcium Phosphate for Orthodontic Adhesive Uses

Nasrin Shahmiri[1], Nahid Hassanzadeh Nemati[1], Ahmad Ramazani Saadatabadi[2], Massoud Seifi[3]*

[1] *Department of Biomedical Engineering, Science and Research Branch, Islamic Azad University, Tehran, Iran.*
[2] *Department of Chemical & Petroleum Engineering, Sharif University of Technology, Tehran, Iran.*
[3] *Department of Orthodontics, School of Dentistry, Shahid Beheshti University of Medical Sciences, Tehran, Iran.*

ARTICLE INFO

Article History:

Received 2024-05-25
Accepted 2024-11-23
Published 2024-02-15

Keywords:

composite resin, orthodontic bonding, white spot lesion, cellulose nanocrystal, amorphous calcium phosphate.

ABSTRACT

White spot lesions (WSLs) commonly develop around orthodontic brackets. Amorphous calcium phosphate (ACP) is known for its remineralizing properties, which can help prevent WSLs. However, the incorporation of ACP may compromise the mechanical strength of the material. This study focuses on the development of experimental orthodontic adhesives incorporating cellulose nanocrystal (CNC) and amorphous calcium phosphate (ACP) to evaluate their bond strength and mineral release properties. The experimental resin formulation included BisEMA, TEGDMA, 4-META, camphorquinone, and DMAEM. Adhesive disks underwent characterization through FE-SEM, EDS, and XRD techniques. The release of minerals was quantified using ICP-OES. The shear bond strength (SBS) was evaluated immediately after bonding metal brackets to bovine incisors. Adhesives containing various fractions of ACP (15%, 20%, and 40%) exhibited sustained release of calcium and phosphorus over a 30-day period. The incorporation of ACP and CNC contributed to a reduction in adhesive cytotoxicity. The adhesive formulation with 40% ACP + 5% CNC showed the lowest SBS, whereas the adhesive with 15% ACP + 5% CNC demonstrated suitable bond strength for orthodontic applications. Addition of 20% CNC to the experimental resin positively impacted bracket bond strength. Likewise, 20% ACP improved shear bond strength. However, the combination of 5% CNC with ACP did not significantly affect bond strength. ACP nanoparticles show promise for integration into experimental orthodontic adhesives containing BisEMA, TEGDMA, 4-META, CQ, and DMAEM. The synergistic use of ACP with CNC remains a topic of debate and warrants further investigation.

How to cite this article
Shahmiri N., Hassanzadeh Nemati N., Ramazani Saadatabadi A., Seifi M., Synthesis of Resin-based Composites Containing Cellulose Nanocrystal and Nano-amorphous Calcium Phosphate for Orthodontic Adhesive Uses. J. Nanoanalysis., 2024; 11(1): 616-635.

*Corresponding Author Email: *nahid_hasanzadeh@yahoo.com*

INTRODUCTION

Tooth enamel, which is composed of long apatite crystals [1], can experience demineralization around orthodontic brackets, leading to the formation of white spot lesions (WSLs) [2]. WSLs are frequently observed in orthodontic patients [3]. To mitigate the risk of WSLs, researchers are exploring the use of remineralizing agents [4]. One approach involves enriching orthodontic adhesive with nanoparticles that contain minerals like calcium (Ca), phosphorus (P), and fluoride (F). These nanoparticles have the potential to inhibit tooth demineralization and promote remineralization, effectively preventing the occurrence of WSLs [5-8].

Polymer-ceramic composites are widely utilized as biomaterials for the repair of bone and tooth defects [9-11]. These versatile materials find applications in dental implants, dental composites, and orthodontic adhesives [12-14]. Specifically, resin-based composites are commonly employed in orthodontic treatments [15]. The incorporation of calcium phosphate into composite structures imparts bioactivity to these materials [16]. While previous studies have predominantly focused on the use of crystalline forms of calcium phosphates in dental applications [17], there has been a shift towards exploring the potential of Amorphous Calcium Phosphate (ACP) in dental resins [18-20]. As a result, several toothpastes based on ACP have been introduced to the market [17]. The dental composites containing small amounts of ACPs have the ability to release significant quantities of Ca and P due to the large surface area of ACPs. This characteristic allows for more fillers to be incorporated into the resin, thus reinforcing its structure [19]. However, it should be noted that an excessive amount of ACP in the adhesive can lead to a reduction in bond strength [7, 8]. For instance, Zhang et al. [7] successfully developed an orthodontic cement by incorporating 40% ACP, which not only exhibited sufficient ion release but also demonstrated adequate shear bond strength (SBS) for orthodontic applications. Their formulation consisted of nano-sized ACP mixed with a resin matrix comprising HEMA, BisGMA, and PMGDM-EBPADMA [7]. However, it is important to note that the use of HEMA as a monomer in dental resins can lead to a weakening of the polymer mechanical properties since HEMA cannot form cross-links [21]. Additionally, HEMA has been found to increase toxicity due to the metabolization of methacrylic acid [22]. The safety of Bis-GMA is also a subject of controversy due to the release of bisphenol-A [23], and these systems are prone to hydrolytic and enzymatic degradation, which can further reduce the strength of bracket bonds [17]. To address these concerns, other monomers such as Bis-EMA (which has a low viscosity), TEGDMA (which exhibits high water sorption properties), and DMAEM (which offers better biocompatibility) can be utilized in dental resins [24]. For example, Aleesa et al. [6] synthesized an orthodontic adhesive containing BisEMA, TEGDMA, DMAEM, Camphorquinone, 4-META, and bioactive glass, which demonstrated long-term release of fluoride, calcium, and phosphate ions while maintaining a satisfactory bracket bond [6]. It should be noted that the resin matrix composition of orthodontic adhesives plays a crucial role in bracket bond strength [7], necessitating the selection of appropriate monomers.

Studies have indicated that orthodontic adhesives containing ACP nanoparticles can achieve acceptable bracket bonding [7, 8, 25]. However, other studies have reported that orthodontic adhesives incorporating ACP exhibit lower bond strength compared to conventional adhesives [14, 26, 27]. The aggregation of ACP particles may contribute to the reduction in mechanical properties of the composite [27, 28]. It has been observed that the inclusion of more

than 40% ACP in the adhesive leads to minimal bond strength despite maximum ion release [8]. To overcome this challenge, the combination of ACP with reinforcing fillers can help optimize the bracket bond without sacrificing ion release. In previous studies, barium boroaluminosilicate glass particles measuring 1.4 μm have been used as reinforcing agents in tandem with ACP [8, 18, 19]. Another potential reinforcing agent is cellulose nanocrystals (CNCs), which are needle- shaped nanoparticles known for their high modulus of elasticity and dimensional stability. The longitudinal tensile modulus of CNCs (145 GPa) exceeds that of Kevlar (130 GPa), suggesting that CNCs have the potential to enhance the mechanical performance of the composite material [29-31]. Wang et al. [32] have reported that CNC/ZnO nanohybrids influence the mechanical properties of dental resin composites. However, more research is needed to fully understand the impact of CNC on the physical characteristics of dental resins [33].

Cellulose/calcium phosphate hybrids have been identified as potential materials for dental repair [34]. Recent advancements in nanotechnology offer new possibilities for eradicating WSLs. One promising approach involves incorporating nanoparticles into adhesives to facilitate the regeneration of tooth enamel [35]. However, it is crucial to develop an orthodontic adhesive that can release mineralizing ions while maintaining sufficient bond strength. Limited research exists on the use of CNC in dental adhesives or the combination of ACP and CNC. In this study, experimental orthodontic adhesives were formulated with ACP as a bioactive filler and CNC as a reinforcing filler to investigate the release of minerals and the bond strength of the bracket. The study aimed to test the following hypotheses: (1) The presence of CNCs influences the bond strength of the experimental adhesive. (2) The presence of ACPs influences the bond strength of the experimental adhesive. (3) The combination of ACPs and CNCs influences the bond strength of the experimental adhesive. (4) The experimental adhesive containing ACP releases Ca and P. (5) The experimental adhesive, which includes ACP with CNC, releases Ca and P.

EXPERIMENTAL

Preparation of the fillers

CNC was synthesized using the acid hydrolysis method as outlined in previous works [36, 37]. The process involved grinding Whatman filter paper and subjecting it to hydrolysis with sulfuric acid. Cold water was used to halt the hydrolysis reaction, followed by removal of the supernatant from the settled solution. The resulting white slurry underwent centrifugation and dialysis. The CNC suspension was sonicated, filtered, and then stored at 4 °C. Prior to freeze-drying, the suspension underwent additional rounds of sonication and filtration. Initially, the suspension was frozen at –80 °C for 24 hours and subsequently dried for 72 hours. The resulting CNC powder was characterized using DLS, AFM, and FE-SEM techniques. Amorphous calcium phosphate (ACP) nanoparticles with a particle size below 150 nm (BET) were procured from Sigma-Aldrich and utilized without further modification.

Preparation of the resin

The resin was prepared utilizing specific monomers detailed in Table 1, based on previous studies [6, 38]. All monomers, sourced from Sigma-Aldrich, were directly used as received. The monomers were accurately weighed and transferred into an aluminum foil-wrapped bottle. A magnetic stirrer was employed to mix all components for 30 minutes at room temperature to ensure a homogeneous blend. The light-sensitive mixture was shielded from light exposure.

Production and characterization of the adhesive disks

The adhesive disks were fabricated following previous studies [6, 38]. The resin and fillers (ACP, CNC) were manually mixed using a spatula. This

adhesive mixture was filled into a metal mold measuring 10 mm in diameter and 1 mm in thickness. Acetate films were positioned above and below the mold, sandwiched between two glass slides. Gravity and pressure were utilized, with 200g weights placed on the glass slides to facilitate the escape of air bubbles and excess adhesive. Each side of the assembly was then cured with an LED light source (GuilinWoodpecker Medical Instrument, LED.D) for 20 seconds per side (40 seconds total). The adhesives were formulated based on previous studies [6, 8, 18-20, 39], yielding the following compositions:

R1: resin (control)

R2: resin + 20% CNC

R3: resin + 15% ACP + 5% CNC

R4: resin + 20% ACP

R5: resin + 40% ACP + 5% CNC

Orthodontic adhesive disks were prepared (Fig. 1), with R1 representing an unfilled resin, designated as the control group. The adhesive disks were characterized using FE-SEM, EDS, and XRD.

Table 1 Methacrylate monomers and the polymerization-initiating components in the experimental resin based on previous studies [6, 38]

Resin Component	Chemical name	Acronym	Content (mass%)
Base monomer	Ethoxylated bisphenol A glycol dimethacrylate	Bis-EMA	42.25
Diluent monomer	Triethylene glycol dimethacrylate	TEGDMA	55
Adhesion promoter monomer	4-methacryloxyethyl trimellitate anhydride	4-META	2
Light cure initiator monomer	Camphorquinone	CQ	0.5
Co-initator & accelerator monomer	Dimethylamino ethyl methacrylate	DMAEM	0.25

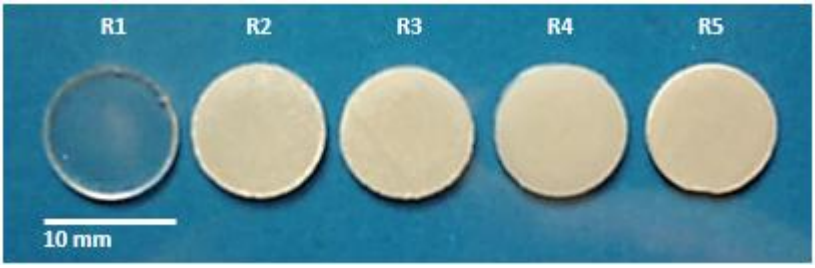

Fig. 1 Experimental adhesive disks: R1 (unfilled resin), R2 (20% CNC), R3 (15% CNC+ 5%ACP), R4 (20% ACP), R5 (40% ACP+5% CNC)

Measurement of Ca and P release

Following a previous study [40], seven disks were prepared for each experimental group. Disks were immersed in 11 ml deionized water within centrifuge tubes, and stored at 37 °C, as described in previous studies [6, 41-43]. The tubes were sealed, and after 30 days, the release of Ca and P was quantified via inductively coupled plasma optical emission spectroscopy (ICP-OES, Spectro, ARCOS).

Cytotoxicity test

Human gingival fibroblast cells (HGF, CELL No. IBRC C10459) were sourced from the Iranian

Biological Resource Center and cultured following previous protocols [44-46]. These cells were maintained in Dulbecco's Modified Eagle Medium (DMEM) and cultivated in a standard incubator. In line with previous methodologies [45, 47], one composite disk measuring 10 mm in diameter and 1 mm in height were fabricated for each experimental group. The top and bottom surfaces of the disks were cured for 20 seconds, followed by UV sterilization of each side of the disks for 30 minutes (totaling 1 hour). Disks were eluted in a culture medium with a surface/volume ratio of 1.25 cm^2/mL [45, 46, 48]. The eluates were incubated for 24 hours, after which the disks were removed, and the extracts were filtered for MTT assay. HGF cells were seeded at a concentration of 1×10^4 cells/mL in a microplate and cultured in the incubator. Subsequently, the cell cultures were exposed to the composite extract, and cytotoxicity levels were evaluated after 24 hours. The MTT solution was introduced into the culture plate, and the cells were incubated. After discarding the supernatant, the formazan crystals were dissolved, and the optical density (OD) was measured at 570 nm. Cell viability was calculated using the formula: (OD of test group / OD of control cells) × 100 [49]. The cytotoxicity outcomes were categorized as severe (≤30%), moderate (30–60%), mild (60–90%), and non-cytotoxic (>90%) based on established criteria [44, 46, 50-52].

Shear bond strength (SBS) and adhesive remnant index (ARI)

Fifty bovine incisors, sourced from a local slaughterhouse (East Livestock Industrial Slaughterhouse, Sari, Iran), were utilized in the study (Fig. 2a). The teeth underwent de-tissueing to remove soft tissues (Fig. 2b) before being embedded in cold-cure acrylic (Acropars Cold-Cure Acrylic, Iran) (Fig. 2c). Based on previous studies [53], ten teeth were assigned to each group for testing different adhesives. Mandibular incisor orthodontic brackets were affixed to the teeth, with all bonding procedures performed by a single operator. The teeth were initially polished using aluminum oxide paste (Dentonext, Iran) and etched with 37% phosphoric acid gel (Condac 37 - FGM, Brazil). A thin layer of adhesive was applied to the mesh of the stainless-steel bracket (IMD, China), which was then positioned near the center of tooth. The adhesive was light-cured for 10 seconds on each side (total of 40 seconds) and immediately subjected to shear force testing using a Universal Testing Machine (Koopa TB-5T, Iran) (Fig. 3) at a crosshead rate of 0.5 mm/min. The maximum force required for bracket detachment was recorded in Newton and converted to MPa [54]. Post-debonding, each tooth was analyzed under a stereomicroscope (Dewinter Technologies) to assess the Adhesive Remnant Index (ARI) based on established criteria [55, 56], specifically:

0: no residual resin on the tooth

1: < 50% resin remaining on the tooth

2: ≥ 50% resin remaining on the tooth

3: 100% resin remaining on the tooth

Statistical analysis

Data analysis was conducted utilizing IBM SPSS Statistics 20 software. Group comparisons were performed using the Kruskal-Wallis test, while pairwise comparisons were assessed using the Mann-Whitney U test [53]. The difference was considered significant when $P \leq 0.05$.

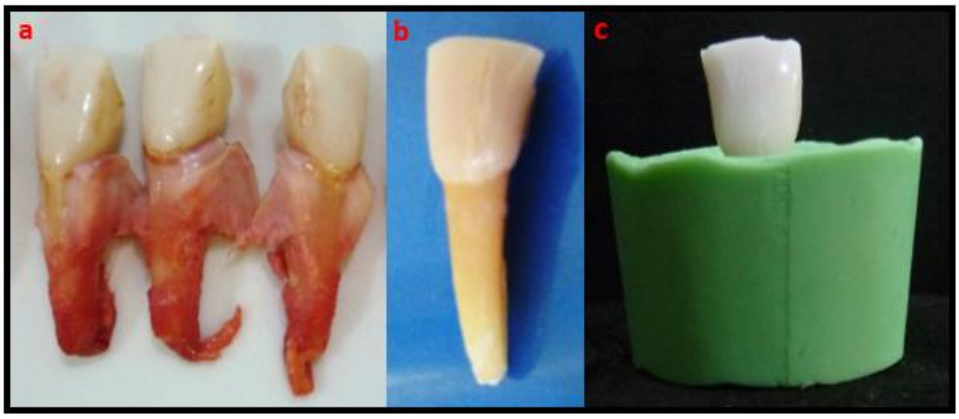

Fig. 2 Preparation of bovine teeth: a) Extraction of mandibular incisors, b) Removal of soft tissue, c) Embedding tooth in cold-cure acrylic

Fig. 3 Placement of tooth for shear bond strength test

RESULTS AND DISCUSSIONS

Characterization of the CNCs

The CNC powder underwent characterization using DLS, AFM, and FE-SEM techniques. The average length of the CNCs was found to be 105.06 ± 7.38 nm based on DLS analysis (Fig. 4).

The morphology of the CNC powder was visualized in Fig. 5a, showing the presence of CNCs. The AFM image in Fig. 5b confirmed the needle-like shape of the CNCs. The FE-SEM image at 500x magnification (Fig. 6a) revealed the flake-like structure of the CNC powder. At a higher magnification of 50000x, the typical rod and needle shapes of the CNCs were observed, providing evidence for successful CNC synthesis (Fig. 6b).

Characterization of the adhesive disks

The FE-SEM image of disk R1 (unfilled resin) is presented in Fig. 7. It also displays the presence of needle-shaped CNCs in the composite as evidenced by the image of disk R2 (20% CNC). Disks R3, R4, and R5 containing nano-ACP showed the presence of spherical ACP nanoparticles, although they were observed to be agglomerated within the matrix (Fig. 7). Elemental composition analysis of disk R1 using EDS revealed the highest amounts of carbon

and nitrogen. This is attributed to the absence of fillers in disk R1, which consisted solely of resin monomers (Table 2). Disk R5 (40% ACP + 5% CNC) had the highest filler content, and EDS analysis

confirmed the elevated levels of calcium and phosphorus in this disk (Table 2). Disk R2 (20% CNC) exhibited the highest amount of oxygen due to the presence of CNCs, which are rich in oxygen (Table 2). Comparatively, disk R4 (20% ACP) contained higher amounts of calcium and phosphorus than disk R3 (15% ACP + 5% CNC) (Table 2). These EDS findings validate the elemental composition consistency of the adhesive disks with their primary theoretical formulation.

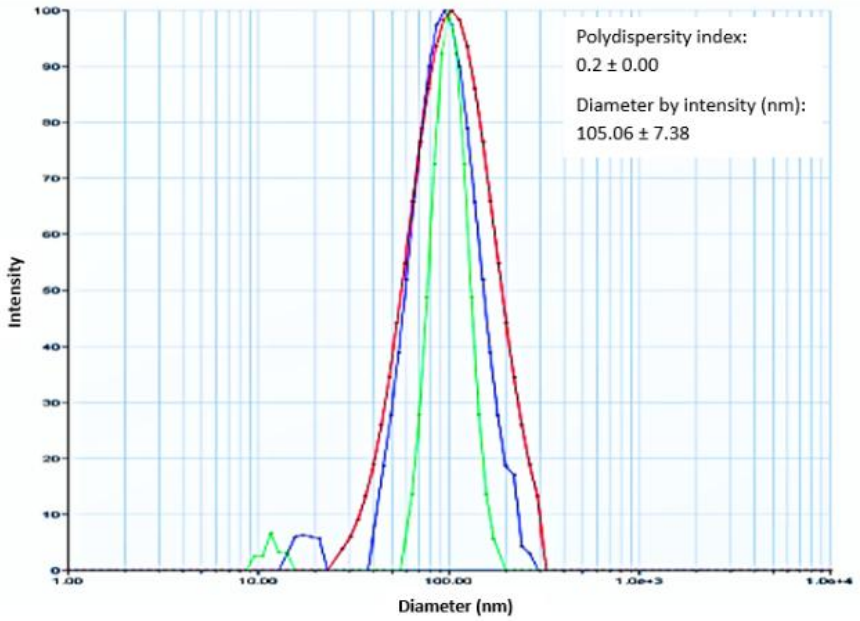

Fig. 4 Size distribution of CNCs obtained from DLS; (Red: first run, Green: second run, Blue: third run)

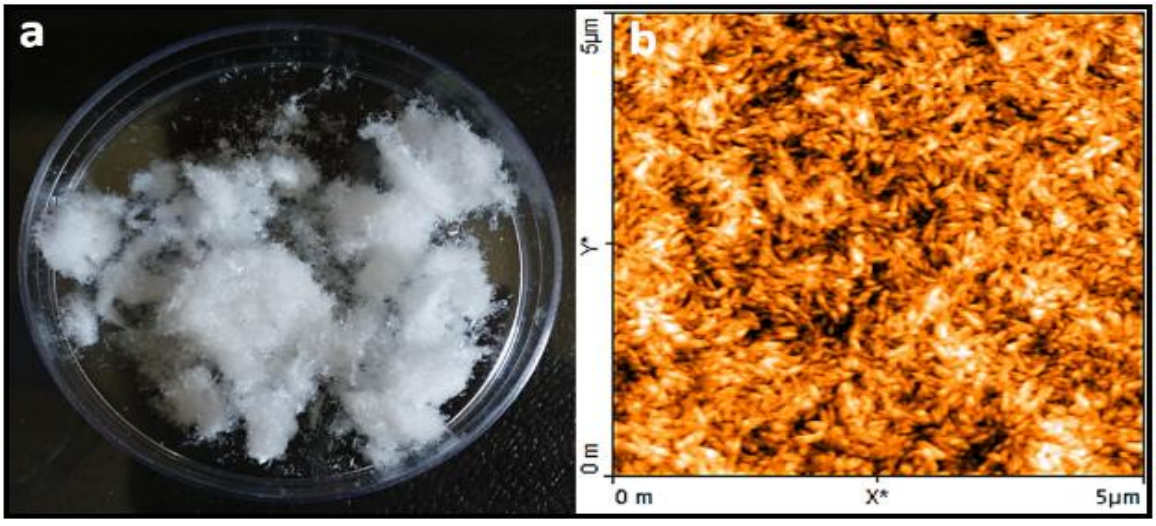

Fig. 5 a) Dry powder of CNC, b) Corresponding AFM image

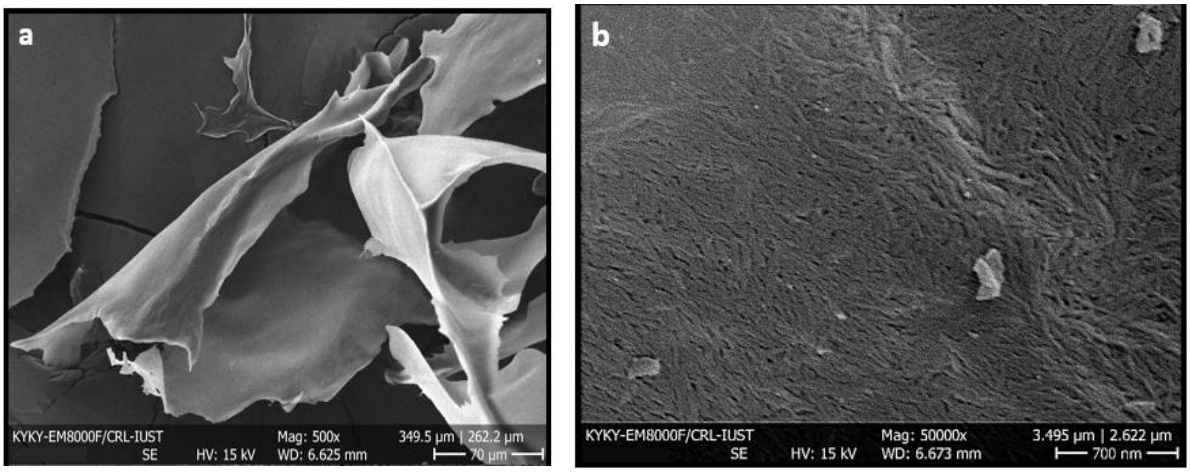

Fig. 6 FE-SEM image of CNC powder: a) 500x magnification, b) 50000x magnification

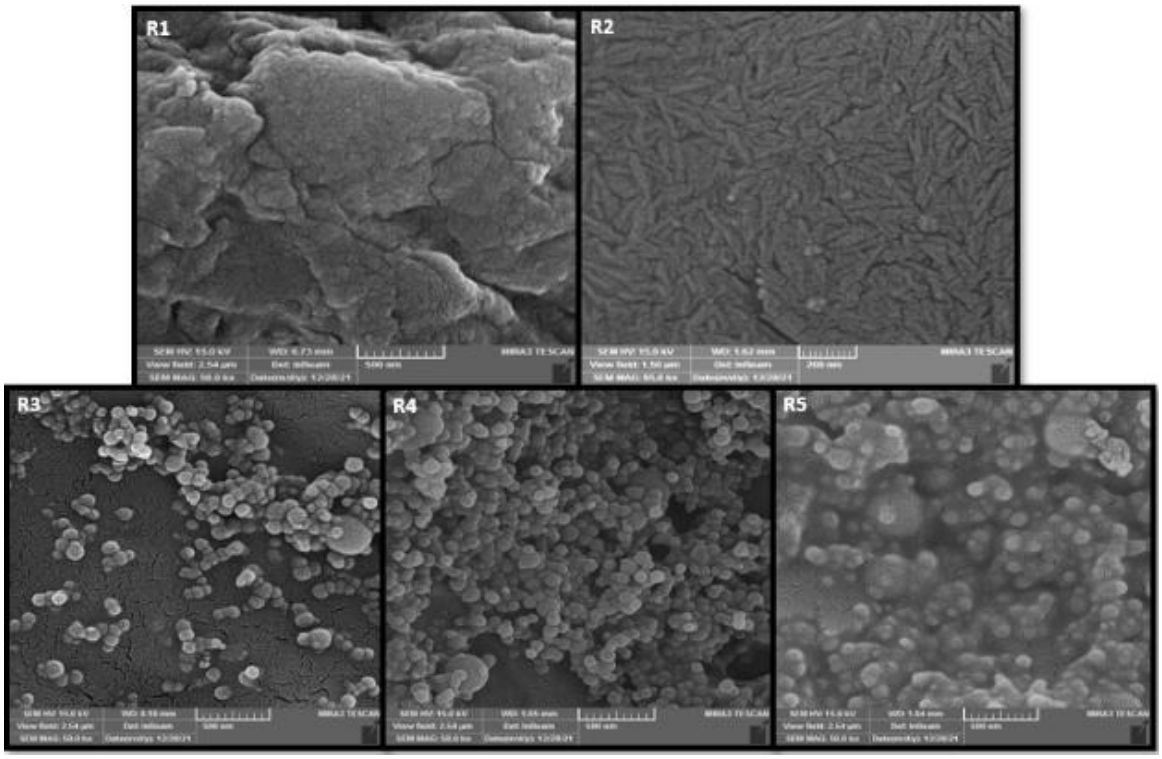

Fig. 7 FE-SEM images of the adhesive disks: R1 (unfilled resin), R2 (20% CNC), R3 (15% CNC + 5% ACP), R4 (20% ACP), R5 (40% ACP + 5% CNC)

Table 2 The elements of the adhesive disks based on EDS analysis
Wt: weight, AT: atomic, R1 (unfilled resin), R2 (20% CNC), R3 (15% CNC + 5% ACP), R4 (20% ACP), R5 (40% ACP + 5% CNC)

Elements	C		O		N		Ca		P	
	Wt%	AT%	Wt%	AT%	Wt%	AT%	Wt%	AT%	Wt%	AT%
R1	62.81	68.92	33.37	27.49	3.82	3.59	-	-	-	-
R2	56.12	63.10	43.57	36.78	-	-	-	-	-	-
R3	54.83	62.49	40.75	34.86	1.57	1.54	1.45	0.49	1.33	0.59
R4	51.85	60.13	41.81	36.40	1.57	1.56	2.36	0.82	2.33	1.05
R5	35.30	47.01	41.70	41.70	1.26	1.44	11.74	4.68	9.82	5.07

The XRD analysis of the disks is presented in Figure 8. The scans were conducted within the 2Θ range of approximately 10-90°. In the XRD pattern of disk R1, two humps can be observed in the 2Θ range of about 10-50°, indicating the presence of the amorphous phase of the resin [57] (Fig. 8). These humps are also visible in the other four disks, albeit with lower intensity. Disk R2 (20% CNC) exhibits a prominent crystalline peak at 2Θ=22.68°, along with smaller peaks at 2Θ=14.75° and 2Θ=16.71°, confirming the presence of CNC based on previous studies [58, 59] (Fig. 8). The XRD pattern of ACP is characterized by two broad humps in the 2Θ range of 20° to 60° [60-62]. In this context, a hump is somewhat visible in disk R3 (15% ACP + 5% CNC) within the 2Θ range of approximately 25-35°, and with lower intensity in disks R4 (20% ACP) and R5 (40% ACP + 5% CNC), indicating the presence of ACP. The peak at 2Θ=22.91° in the pattern of disk R3 confirms the presence of CNC. Likewise, the peak at 2Θ= 22.60° confirms the presence of CNC in disk R5. The patterns of disks R3, R4, and R5 exhibit two crystalline peaks at approximately 2Θ=26° and 3 2Θ=40°, which may be attributed to the crystallization of ACP particles. Premature crystallization poses a significant challenge in handling ACP particles, as studies have shown that ACP powder can transform into crystalline hydroxyapatite within a few hours at room temperature [63, 64]. ACP tends to crystallize rapidly under both wet and dry conditions [63, 65]. However, the XRD patterns of disks R3, R4, and R5 do not align with crystalline phases such as apatite or octacalcium phosphate, suggesting that the ACP particles were not fully crystallized. Overall, the XRD patterns (Fig. 8) are consistent with the components of the adhesive disks.

Mineral release

The adhesive disks were evaluated for the release of Ca and P following a 30-day immersion period (Fig. 9). Disk R5 (40% ACP + 5% CNC) demonstrated the highest Ca and P release compared to Disk R3 (15% ACP + 5% CNC) and Disk R4 (20% ACP), with statistically significant differences (P = 0.002). Moreover, Disk R4 exhibited a greater Ca release than Disk R3, with a significant difference (P = 0.048). Similarly, the P release from Disk R4 surpassed that of Disk R3, with a statistically significant difference (P = 0.035) (Fig. 9).

Adhesive R5 (40% ACP + 5% CNC) demonstrated higher calcium (Ca) and phosphorus (P) release when compared to R3 (15% ACP + 5% CNC) and R4 (20% ACP) (Fig. 9), a finding consistent with previous studies [7, 8, 17, 20]. Skrtic et al. [66] highlighted the critical role of filler quantity in determining ion release capacity, noting a significant increase in Ca and P release at specific ACP content thresholds (0.37 to 0.40) [66]. In this study, there was a sharp escalation in Ca and P release as ACP content rose from 0.15 to 0.40 (Fig. 9). Higher ACP content in adhesives promotes water and ion diffusion by enhancing interface availability [8]. The nano-sized ACPs, with their extensive surface area and strong water affinity, facilitate rapid mineral release [7, 17, 19]. ACP content exceeding 40% was deemed impractical in this study as it resulted in overly dry adhesives. While the Ca and P release from adhesives R3 (15% ACP + 5% CNC) and R4 (20% ACP) did not exhibit significant levels, it provides valuable insights into mineral release from the experimental resin. Aleesa et al. [38] highlighted that a composite containing bioactive glass in a neutral solution has a subdued reaction but can induce apatite precipitation in Ca and PO_4 ion-enriched solutions. Given that disk R5 (40% ACP + 5% CNC) released the highest levels of Ca and P (Fig. 9), it holds promise for apatite formation in neutral solutions. ACPs are known to transition from volatile states to crystalline CaPs in solutions, suggesting potential tooth mineral regeneration

through ACP composites [17, 67]. Therefore, the mineral loss of teeth can be regenerated by the use of ACP composites [68, 69]. It is postulated that ACP/CNC particle distribution was uneven in this study. During the water absorption and ion release process, the filler-resin matrix interfaces were subject to unpredictable spatial variations [70].

In this study, triethylene glycol dimethacrylate (TEGDMA) was introduced into the resin to regulate viscosity, boasting a degree of hydrophilicity leading to water absorption. On the other hand, ethoxylated bisphenol A glycol dimethacrylate (Bis-EMA) exhibited lower viscosity and hydrophilicity [71, 72]. Polymerization was initiated using a free radical mechanism involving camphoroquinone (CQ), with an accelerator like dimethylaminoethyl methacrylate (DMAEM) included [73-75]. The ion release kinetics from the adhesive disks (R3-R5) were chiefly influenced by the TEGDMA monomer content, as its hydrophilic nature aids water absorption, ion diffusion, and potentially internal mineral saturation [17, 22, 73-75]. Moreover, the experimental adhesives featured 4-methacryloxyethyl trimellitate anhydride (4-META), which may enhance the composite-to-tooth bond by acting as a chelator of calcium ions and improving enamel surface wetting [76, 77], potentially impacting calcium release.

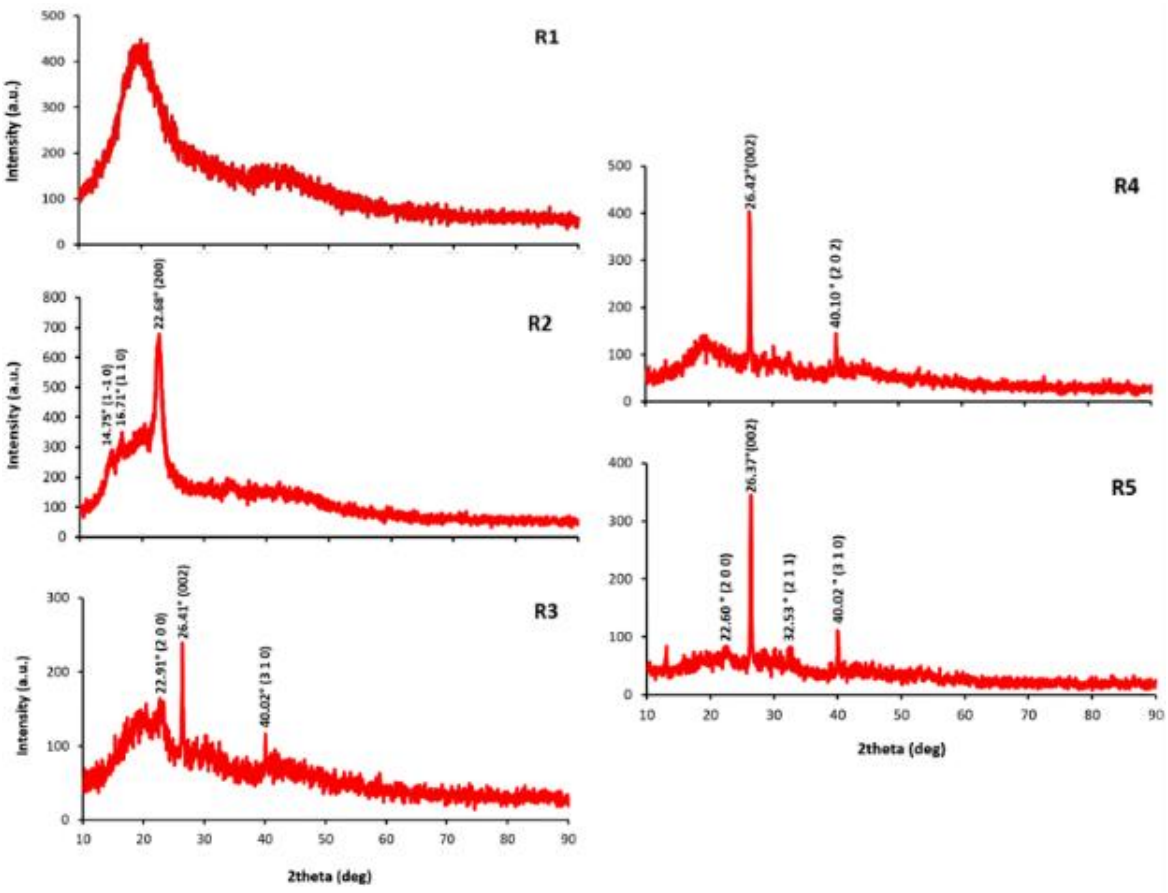

Fig. 8 XRD patterns of the adhesive disks: R1 (unfilled resin), R2 (20% CNC), R3 (15% CNC + 5%ACP), R4 (20% ACP), R5 (40% ACP + 5% CNC)

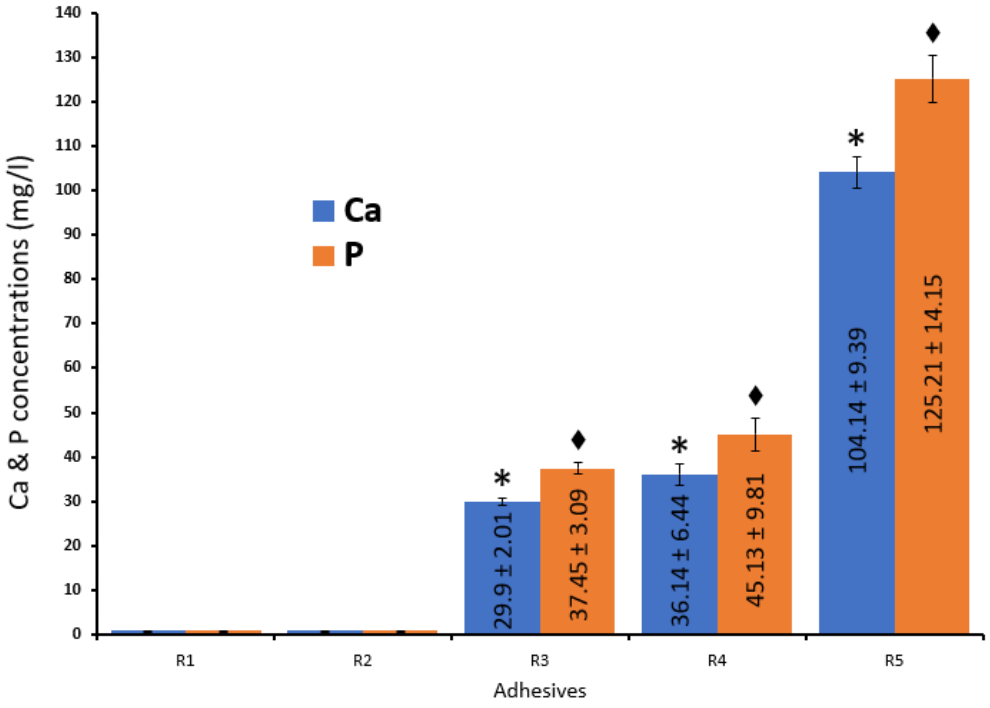

Fig. 9 Average Ca and P release (Mean ± SD) from adhesive disks after 30 days. Symbols (*♦) indicate pairwise significant differences between groups ($P < 0.05$). R1 (unfilled resin), R2 (20% CNC), R3 (15% CNC + 5% ACP), R4 (20% ACP), R5 (40% ACP + 5% CNC)

Cell viability

Cell viability was lower for all adhesive disks in contrast to the pure medium, with statistical significance ($P = 0.05$), except for disk R4 (20% ACP) (Fig. 10). This suggests that disk R4 displayed superior biocompatibility among the adhesive disks. Notably, the cell viability post-exposure to disk R1 (unfilled resin) was 61.3 ± 0.8%, indicating mild toxicity. In comparison, adhesive R2 (20% CNC) demonstrated a cell viability of 86.9%, signaling low toxicity attributed to cellulose nanocrystals (Fig. 10).

In Fig. 11, the appearance of HGF cells post-exposure to the composite extracts is depicted. Mediums R1 (unfilled resin) and R2 (20% CNC) showcased more cells with spherical shapes, implying a distinct cellular response compared to mediums R3 (15%ACP+5%CNC), R4 (20%ACP), and R5 (40%ACP+5%CNC), where cells exhibited predominantly polygonal and spread shapes similar to those in the pure medium (Fig. 11a). The presence of polygonal and spread cell shapes in mediums R3, R4, and R5 signifies the biocompatibility of ACP nanoparticles, as evidenced by cellular morphology akin to that of healthy cells. The microscopic observations align with the Elisa reader outcomes (Fig. 10 & 11). To mitigate toxicity, nanoparticles were incorporated into the resin, although further research is warranted to confirm the safety of cellulose nanocrystals (CNC) for clinical applications. Menezes-Silva et al. [78] successfully enhanced the biocompatibility of commercial glass ionomer cement (GIC) by incorporating CNC.

SBS & ARI assessment

Significant differences were observed in the mean SBS of the control adhesive (R1: unfilled resin) compared to other experimental groups ($P < 0.05$) (Fig. 12), suggesting diverse adhesive performances. No substantial difference was noted in the bond strength between adhesive R2 (20% CNC) and R3 (15% ACP + 5% CNC) ($P = 0.199$) (Fig. 12). While the mean SBS of adhesive R4 (20% ACP) exceeded that of R2 (20% CNC), the distinction was not statistically significant

(P= 0.096) (Fig. 12). Adhesive R5 (40% ACP + 5% CNC) demonstrated the lowest SBS among the groups, with a statistically significant difference (P < 0.01), indicative of a weaker bond when compared to other formulations.

In terms of bonding strength, the composite resin displayed a range of 2 to 13 MPa with metal brackets in previous studies [79]. Adhesive R1 (pure resin) demonstrated a reasonably strong bond strength of approximately 10 MPa, indicating that Bis-EMA and TEGDMA in combination form a robust bond with enamel (Fig. 12). The mechanical functionality of adhesives R3 (15% ACP + 5% CNC), R4 (20% ACP), and R5 (40% ACP + 5% CNC) containing ACP is predominantly influenced by the irregular distribution of ACP clusters rather than the composition of the resin [17, 80]. Skrtic et al. [70] integrated Zr-ACP particles into dental resin, with a median particle diameter of 8.6 ± 2.4 µm. They suggested that reducing the size of ACP particles enhances the interaction between ACP and resin, thereby improving the mechanical strength of the composite [70]. In this study, nano-sized ACP particles (<150 nm) were utilized, potentially impacting the shear bond strength (Fig. 12). Furthermore, Skrtic et al. [66] noted that amorphous calcium phosphate could weaken the filled polymer compared to the unfilled polymer. The inherent aggregation of ACP particles weakens ACP/resin interactions, leading to the destabilization of the filler/polymer interface and reduced mechanical strength [17, 27, 62], limiting the use of ACP-based composites to non-stress-bearing applications like fissure sealants [14, 17, 69, 80]. Unexpectedly, adhesives R3 (15% ACP + 5% CNC) and R4 (20% ACP) exhibited higher shear bond strength than the unfilled resin (R1) in this study (Fig. 12). This enhanced strength in adhesives R3 and R4 (Fig. 12) can be attributed to the incorporation of nano-sized ACP and CNC. Nano-ACPs offer a larger surface area, providing more room within the polymer matrix for incorporating reinforcing fillers and enhancing mechanical properties [8]. However, adhesive R5 (40% ACP & 5% CNC) displayed an SBS of approximately 6 MPa, the minimum acceptable bond strength that could result in premature bracket debonding during treatment [8] (Fig. 12). It is hypothesized that the heterogeneous ACP/CNC fillers could not establish a close interlocking network with the experimental resin. Optimal CNC content within the resin can create a permeated network, as seen with the incorporation of 20% CNC (R2), yielding a suitable shear bond strength (Fig. 12). Past research has demonstrated that CNC can effectively enhance the mechanical properties of dental resins [32, 81]. Sabir et al. [81] successfully enhanced the mechanical properties of dental adhesive by incorporating CNC. Likewise, Moradian et al. [82] discovered that incorporating bacterial CNC into resin-modified glass ionomer cement (RMGICs) can improve shear bond strength properties.

There were no substantial differences in ARI values between the control adhesive (R1) and the other experimental groups (P > 0.05) (Fig. 13), suggesting similar patterns of adhesive residue distribution post-bond failure.

The performance of composites is influenced by the type of filler, filler quantity, and resin composition [83]. An effective adhesive must not only endure the functional stresses in the oral cavity but also safeguard oral tissues from damage [84]. The high Adhesive Remnant Index (ARI) scores observed in this study (Fig. 13) could impact the enamel post-orthodontic treatment. A higher amount of adhesive remnant necessitates additional enamel polishing to eliminate the adhesive residue after bracket debonding [85]. Nonetheless, there is conflicting information in the literature regarding ARI scores. A greater presence of adhesive remnants on the enamel suggests bracket debonding occurs at the bracket/adhesive interface, preventing enamel chipping and fracturing [85-88]. In our investigation, the elevated ARI scores across all adhesives correlated with increased bond strength, with

the exception of adhesive R5 (Fig. 12 & 13). A high ARI score (2 & 3), indicative of greater bond strength, could be advantageous in orthodontic applications [85, 88, 89].

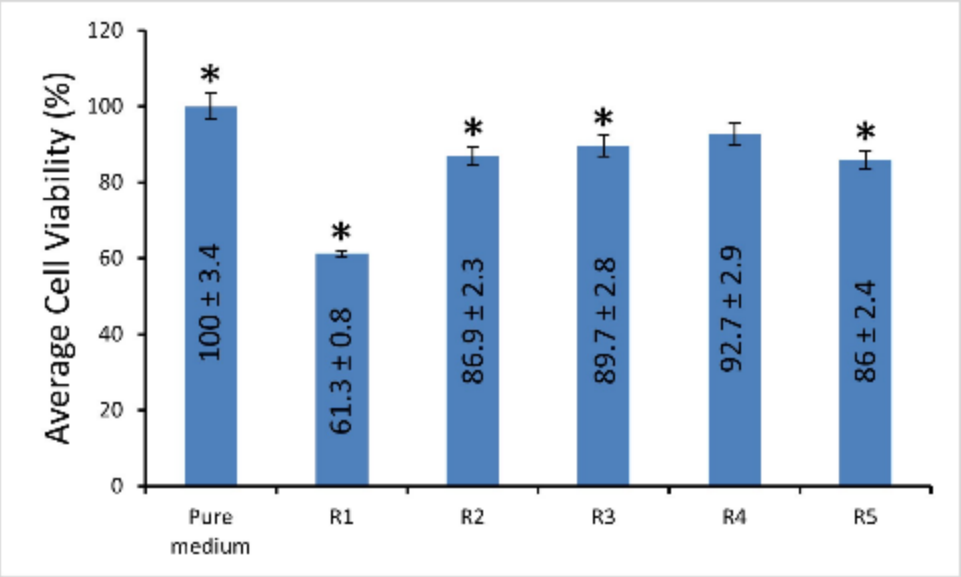

Fig. 10 Results of MTT assay after 24 h. Symbol (*) denotes significant differences between pure medium (untreated cells) and adhesive disks ($P = 0.05$). R1 (unfilled resin), R2 (20% CNC), R3 (15% CNC + 5% ACP), R4 (20% ACP), R5 (40% ACP + 5% CNC)

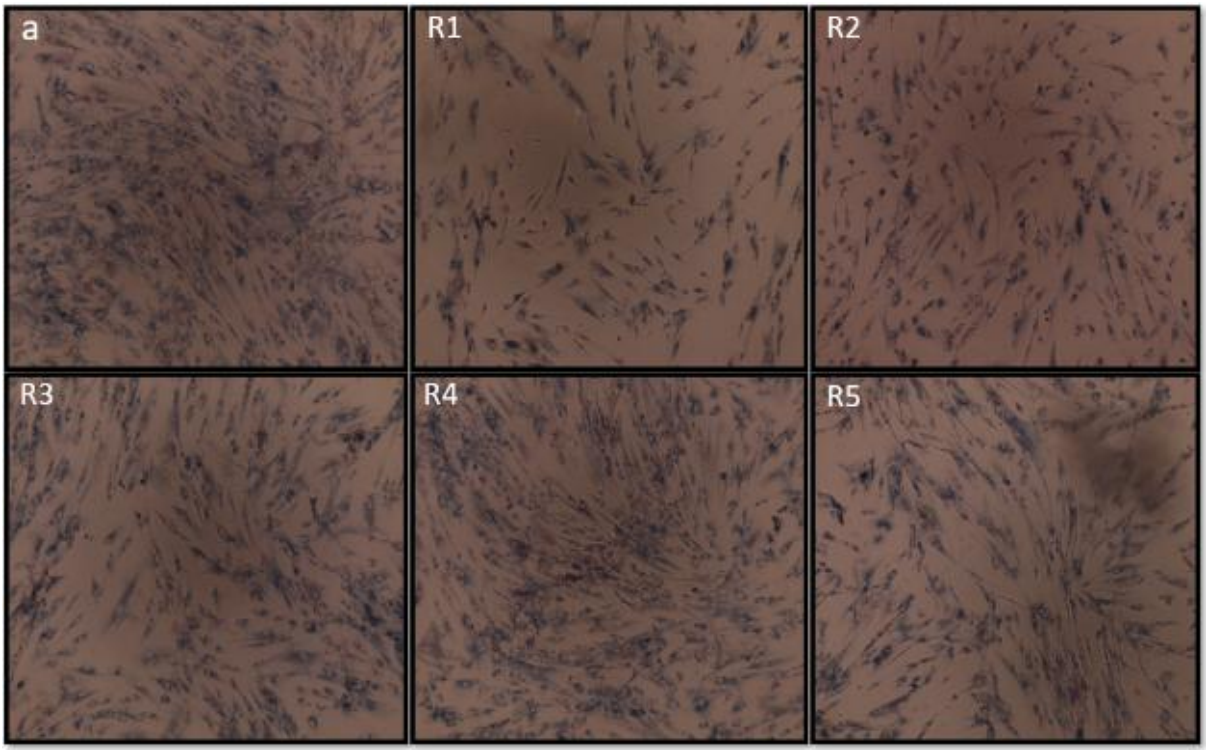

Fig. 11 Optical micrographs of HGF cells post exposure to extracts from adhesive disks. a) Pure medium (untreated cells), R1 (unfilled resin), R2 (20% CNC), R3 (15% CNC + 5% ACP), R4 (20% ACP), R5 (40% ACP + 5% CNC)

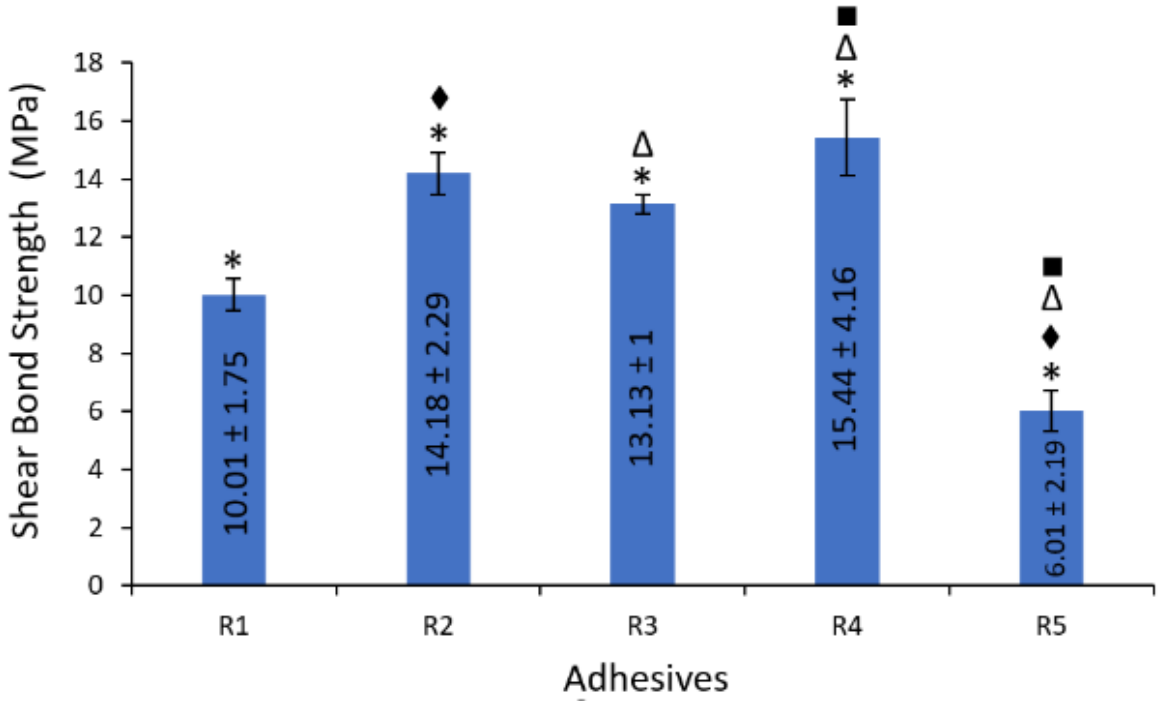

Fig. 12 Shear bond strength (Mean ± SD) of experimental adhesives. Symbol (*) indicates significant differences between R1 (control) and other groups ($P < 0.05$). Symbols (♦Δ■) represent pairwise significant differences between groups ($P < 0.05$). R1 (unfilled resin), R2 (20% CNC), R3 (15% CNC + 5% ACP), R4 (20% ACP), R5 (40% ACP + 5% CNC)

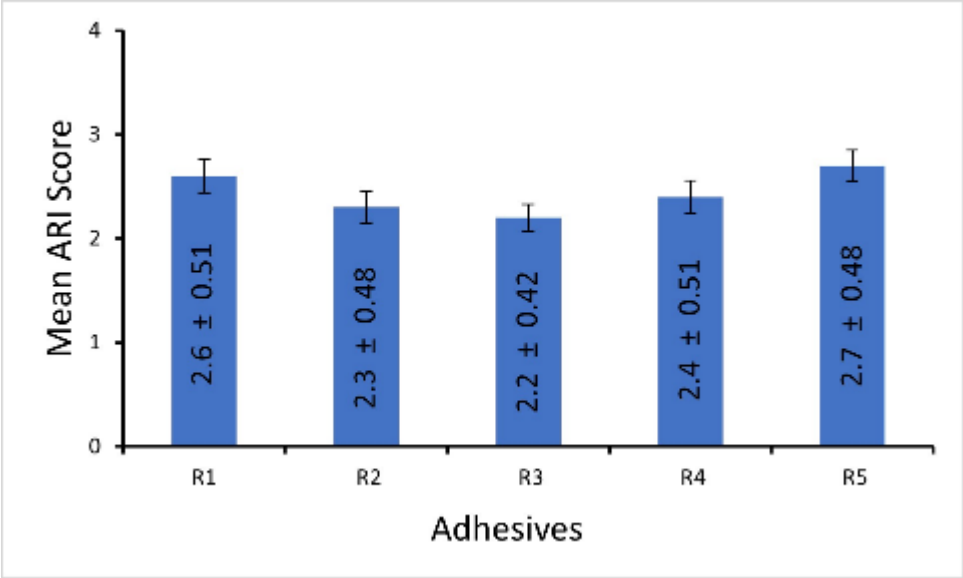

Fig. 13 Average ARI (Adhesive Remnant Index) score (Mean ± SD) based on adhesive remnants on tooth after bracket debonding. R1 (unfilled resin), R2 (20% CNC), R3 (15% CNC + 5% ACP), R4 (20% ACP), R5 (40% ACP + 5% CNC)

CONCLUSION

The effects of incorporating ACP and CNC into an experimental resin were investigated for orthodontic use. The adhesive R2, which contained 20% CNC, had a suitable shear bond strength for orthodontic applications. Adhesive R4, which contained 20% ACP, released calcium and phosphorus and also provided acceptable shear bond strength. Adhesive R3, a combination of 15% ACP and 5% CNC, released calcium and phosphorus but had a lower shear bond

strength compared to R4. Adhesive R5, with 40% ACP and 5% CNC, had the highest mineral release but the lowest shear bond strength. The incorporation of ACP into the experimental resin showed promise for orthodontics and prevention of white spot lesions (WSLs). However, the addition of 5% CNC alongside ACP did not significantly affect the bracket bond strength. Further experiments are needed to confirm the therapeutic benefits of ACP and the mechanical properties of CNC in resin-based orthodontic adhesives.

CONFLICT OF INTEREST

The authors declare that they have no conflicts of interest.

FUNDING

This research did not receive any specific grant from funding agencies in the public, commercial, or not-for-profit sectors.

REFERENCES

1. Pandya M and Diekwisch T. Enamel biomimetics—fiction or future of dentistry. Int J Oral Sci 2019; 11:8.
2. Bishara S and Ostby A. White Spot Lesions: Formation, Prevention, and Treatment. Semin Orthod 2008; 14:174-182.
3. Twomley J, Yu Q, Ballard R, Armbruster P and Xu X. Formulation and characterization of antibacterial orthodontic adhesive. Dental Press J Orthod 2019; 24:73-9.
4. Walsh LJ and Healey DL. Prevention and caries risk management in teenage and orthodontic patients. Aust Dent J 2019; 64:S37-S45.
5. Nam HJ, Kim YM, Kwon YH, Kim IR, Park BS, Son WS, Lee SM and Kim YI. Enamel Surface Remineralization Effect by Fluorinated Graphite and Bioactive Glass-Containing Orthodontic Bonding Resin. Materials 2019; 12:1308.
6. Al-eesa NA, Wong FSL, Johal A and Hill RG. Flouride containing bioactive glass composite for orthodontic adhesives - ion release properties. Dent Mater 2017; 33:1324-29.
7. Zhang L, Weir MD, Chow LC, Reynolds MA and Xu HHK. Rechargeable calcium phosphate orthodontic cement with sustained ion release and re-release. Sci Rep 2016; 6:36476.
8. Xie X, Wang L, Xing D, Qi M, Li X, Sun J, Melo MAS, Weir MD, Oates TW, Bai Y and Xu HHK. Novel rechargeable calcium phosphate nanoparticle-filled dental cement. Dent Mater J 2019; 38:1-10.
9. Haghani N, Hassanzadeh Nemati N, Khorasani MT and Bonakdar S. Fabrication of polycaprolactone/heparinized nano fluorohydroxyapatite scaffold for bone tissue engineering uses. Int J Polym Mater Polym Biomater 2023.
10. Hassanzadeh Nemati N and Mirhadi SM. Study on polycaprolactone coated hierarchical meso/macroporous Titania scaffolds for bone tissue engineering. Int J Eng 2022; 35:1887-1894.
11. Lee JH, Kim HW and Seo SJ. Polymer-Ceramic Bionanocomposites for Dental Application. J Nanomater 2016; 2016:3795976.
12. Greenberg AR and Kamel I. Polymer-ceramic composite for tooth-root implant. J Biomed Mater Res 1976; 10:777-788.
13. Xie C, Zhang JF and Li S. Polymer Infiltrated Ceramic Hybrid Composites as Dental Materials. Oral Health Dent Stud 2018; 1:2.

14. Dunn WJ. Shear bond strength of an amorphous calcium-phosphate–containing orthodontic resin cement. Am J Orthod Dentofacial Orthop 2007; 131:243-7.
15. Wang WN and Meng CL. A study of bond strength between light-and self-cured orthodontic resin. Am J Orthod Dentofacial Orthop 1992; 101:350-4.
16. Rahnejat B, Hassanzadeh Nemati N, Sadrnezhaad SK and Shokrgozar MA. Promoting osteoblast proliferation and differentiation on functionalized and laser treated titanium substrate using hydroxyapatite/β-tricalcium phosphate/silver nanoparticles. Mater Chem Phys 2023; 293:126885.
17. Bienek DR, Giuseppetti AA and Skrtic D. Amorphous Calcium Phosphate as Bioactive Filler in Polymeric Dental Composites, in Calcium Phosphates - From Fundamentals to Applications. IntechOpen 2019.
18. Melo MAS, Weir MD, Rodrigues LKA and Xu HHK. Novel calcium phosphate nanocomposite with caries-inhibition in a human in situ model. Dent Mater 2013; 29:231-240.
19. Xu HHK, Moreau JL, Sun L and Chow LC. Nanocomposite containing amorphous calcium phosphate nanoparticles for caries inhibition. Dent Mater 2011; 27:762-9.
20. Chen C, Weir MD, Cheng L, Lin N, Lin-Gibson S, Chow LC, Zhou X and Xu HHK. Antibacterial activity and ion release of bonding agent containing amorphous calcium phosphate nanoparticles. Dent Mater 2014; 30:891-901.
21. Par M, Tarle Z, Hickel R and Ilie N. Real-time curing characteristics of experimental resin composites containing amorphous calcium phosphate. Eur J Oral Sci 2018; 126:426-432.
22. Durner J, Walther UI, Zaspel J, Hickel R and Reich FX. Metabolism of TEGDMA and HEMA in human cells. Biomaterials 2010; 31:818-823.
23. Yin M, Liu F and He J. Preparation and characterization of Bis-GMA free dental resin system with synthesized dimethacrylate monomer TDDMMA derived from tricyclo[5.2.1.0(2,6)]-decanedimethanol. J Mech Behav Biomed Mater 2016; 57:157-163.
24. Pratap B, Gupta RK, Bhardwaj B and Nag M. Resin based restorative dental materials: characteristics and future perspectives. Jpn Dent Sci Rev 2019; 55:126-138.
25. Xie XJ, Xing D, Wang L, Zhou H, Weir MD, Bai YX and Xu HH. Novel rechargeable calcium phosphate nanoparticle containing orthodontic cement. Int J Oral Sci 2017; 9:24-32.
26. Foster JA, Berzins DW and Bradley TG. Bond strength of an amorphous calcium phosphate- containing orthodontic adhesive. Angle Orthod 2008; 78:339-344.
27. Zhao J, Liu Y, Sun WB and Zhang H. Amorphous calcium phosphate and its application in dentistry. Chem Cent J 2011; 5:40.
28. Schumacher GE, Antonucci JM, O'Donnell JN and Skrtic D. The use of amorphous calcium phosphate composites as bioactive basing materials: their effect on the strength of the composite/adhesive/dentin bond. J Am Dent Assoc 2007; 138:1476-1484.
29. Yang Y, Chen Z, Zhang J, Wang G, Zhang R and Suo D. Preparation and Applications of the Cellulose Nanocrystal. Int J Polym Sci 2019; 2019:1767028.
30. Sturcova A, Davies GR and Eichhorn SJ. The elastic modulus and stress-transfer properties

of tunicate cellulose whiskers. Biomacromolecules 2005; 6:1055-1061.

31. Lahiji RR, Reifenberger R, Raman A, Rudie A and Moon RJ. Characterization of Cellulose Nanocrystal Surfaces by SPM. NSTI-Nanotech 2008; 2:704-7.
32. Wang Y, Hua H, Li W, Wang R, Jiang X and Zhu M. Strong antibacterial dental resin composites containing cellulose nanocrystal/zinc oxide nanohybrids. J Dent 2019; 80:23-9.
33. Leite A, Viotto H, Nunes T, Pasquini D and Pero A. Cellulose nanocrystals into Poly(ethylmethacrylate) used for dental application. Polímeros 2022; 32:e2022006.
34. Salama A. Cellulose/calcium phosphate hybrids: New materials for biomedical and environmental applications. Int J Biol.Macromol 2019; 127:606-617.
35. Luminiţa Cosma L, Şuhani RD, Mesaroş A and Eugenia Badea M. Current treatment modalities of orthodontically induced white spot lesions and their outcome – a literature review. Med Pharm Rep 2019; 92:25-30.
36. Shahmiri N, Hassanzadeh Nemati N, Ramazani Saadatabadi A and Seifi M. Cellulose Nanocrystal (CNC) Synthesis: An AFM Study. J Nanostruct 2021; 11:684-697.
37. Shahmiri N, Hassanzadeh Nemati N, Ramazani Saadatabadi A and Seifi M. The effect of acid/cellulose ratio on the quality of Cellulose Nanocrystal (CNC) suspension. J Nanoanalysis 2022.
38. Al-eesa NA, Johal A, Hill RG and Wong FSL. Flouride containing bioactive glass composite for orthodontic adhesives__ Apatite formation properties. Dent Mater 2018; 34:1127-1133.
39. Xu HHK, Weir MD, Sun L, Takagi S and Chow LC. Effects of Calcium Phosphate Nanoparticles on Ca-PO4 Composite. J Dent Res 2007; 86:378-383.
40. Chanachai S, Chaichana W, Insee K, Benjakul S, Aupaphong V and Panpisut P. Physical/Mechanical and Antibacterial Properties of Orthodontic Adhesives Containing Calcium Phosphate and Nisin. J Funct Biomater 2021; 12:73.
41. Pires-de-Souza FCP, Moraes PC, Garcia LFR, Aguilar FG and Watanabe E. Evaluation of pH, calcium ion release and antimicrobial activity of a new calcium aluminate cement. Braz Oral Res 2013; 27:324-330.
42. Ghazvini SA, Tabrizi MA, Kobarfard F, Baghban AA and Asgary S. Ion release and pH of a new endodontic cement, MTA and Portland cement. Int Endod J 2009; 4:74-8.
43. Galal M, Zaki DY, Rabie MI, El-Shereif SM and Hamdy TM. Solubility, pH change, and calcium ion release of low solubility endodontic mineral trioxide aggregate. Bull Natl Res Cent 2020; 44:42.
44. Pourhajibagher M, Ghorbanzadeh R, Salehi-Vaziri A and Bahador A. In Vitro Assessments of Antimicrobial Potential and Cytotoxicity Activity of an Orthodontic Adhesive Doped with Nano-Graphene Oxide. Folia Med 2022; 64:110-116.
45. Bationo R, Rouamba A, Diarra A, Beugré-Kouassi MLK, Beugré JB and Jordana F. Cytotoxicity evaluation of dental and orthodontic light-cured composite resins. Clin Exp Dent 2021; 7:40-48.
46. Beltrami R, Colombo M, Rizzo K, Cristofaro AD, Poggio C and Pietrocola G. Cytotoxicity of Different Composite Resins on Human Gingival Fibroblast Cell Lines. Biomimetics 2021; 6:26.
47. Lee SM, Yoo KH, Yoon SY, Kim IR, Park BS, Son WS, Ko CC, Son SA and Kim YI.

Enamel Anti-Demineralization Effect of Orthodontic Adhesive Containing Bioactive Glass and Graphene Oxide: An In-Vitro Study. Materials(Basel) 2018; 11:1728.

48. Cao T, Saw TY, Heng BC, Liu H, Yap AUJ and Ng ML. Comparison of different test models for the assessment of cytotoxicity of composite resins. J Appl Toxicol 2005; 25:101-108.
49. Vande Vannet B, Mohebbian N and Wehrbein H. Toxicity of used orthodontic archwires assessed by three-dimensional cell culture. Eur J Orthod 2006; 28:426-432.
50. Goldberg M. In vitro and in vivo studies on the toxicity of dental resin components: A review. Clin Oral Investig 2008; 12:1-8.
51. Geurtsen W, Lehmann F, Spahl W and Leyhausen G. Cytotoxicity of 35 dental resin composite monomers/additives in permanent 3T3 and three human primary fibroblast cultures. J Biomed Mater Res 1998; 41:474-480.
52. Al-Hiyasat AS, Darmani H and Milhem MM. Cytotoxicity evaluation of dental resin composites and their flowable derivatives. Clin Oral Investig 2005; 9:21-5.
53. Blanchard AB, Mon HH, Wang Y, Chapple A, Dupree P, Ballard R and et al. Formulation and characterization of experimental orthodontic adhesive containing antibacterial dimethacrylate DABCO monomers: An in vitro study. Int orthod 2022; 20:100706.
54. Tavares SW, Consani S, Nouer DF, Magnani MB, Nouer PR and Martins LM. Shear bond strength of new and recycled brackets to enamel. Braz Dent J 2006; 17:44-8.
55. Schaneveldt S and Foley TF. Bond strength comparison of moisture-insensitive primers. Am J Orthod Dentofac Orthop 2002; 122:267-273.
56. Tessore E, Mazzotta L and Fortini A. Evaluation of shear bond strength and adhesive remnant index of orthodontic brackets bonded directly or indirectly with adhesive resin cements to bovine enamel. J Dent Health Oral Disord Ther 2017; 8:521-6.
57. Li A, Cui Y, Gao S, Li Q, Xu L, Meng X, Dong Y, Liu X and Qiu D. Biomineralizing Dental Resin Empowered by Bioactive Amphiphilic Composite Nanoparticles. ACS Appl Bio Mater 2019; 2:1660-66.
58. Trilokesh C and Uppuluri KB. Isolation and characterization of cellulose nanocrystals from jackfruit peel. Sci Rep 2019; 9:16709.
59. Abiaziem CV, Williams AB, Inegbenebor AI, Onwordi CT, Ehi-Eromosele CO and Petrik LF. Isolation and characterisation of cellulose nanocrystal obtained from sugercane peel. Rasayan J Chem 2020; 13:177-187.
60. Vecbiskena L, Gross A, Riekstina U and Yang TCK. Crystallized nano-sized alpha-tricalcium phosphate from amorphous calcium phosphate: microstructure, cementation and cell response. Biomed Mater 2015; 10:025009.
61. Ramalingam M, Young MF, Thomas V, Sun L, Chow LC, Tison CK, Chatterjee K, Miles WC and Jr CGS. Nanofiber scaffold gradients for interfacial tissue engineering. J Biomater Appl 2012; 27:695-705.
62. Zhao J, Liu Y, Sun WB and Yang X. First detection, characterization, and application of amorphous calcium phosphate in dentistry. J Dent Sci 2012; 7:316-323.
63. Esposti LD, Markovic S, Ignjatovic N, Panseri S, Montesi M, Adamiano A, Fosca M, Rau JV, Uskokovic V and Iafisco M. Thermal crystallization of amorphous calcium phosphate combined with citrate and fluoride doping: a novel route to produce

hydroxyapatite bioceramics. J Mater Chem B 2021; 9:4832–4845.

64. Dorozhkin SV. Amorphous calcium (ortho)phosphates. Acta Biomater 2010; 6:4457-4475.
65. Boskey AL and Posner AS. Conversion of amorphous calcium phosphate to microcrystalline hydroxyapatite. A pH-dependent, solution-mediated, solid-solid conversion. J Phys Chem 1973; 77:2313–17.
66. Skrtic D, Antonucci JM and Eanes ED. Improved properties of amorphous calcium phosphate fillers in remineralizing resin composites. Dent Mater 1996; 12:295-301.
67. O'Donnell JNR, Antonucci JM and Skrtic D. Illuminating the role of agglomerates on critical physicochemical properties of amorphous calcium phosphate composites. J Compos Mater 2008; 42:2231-2246.
68. Skrtic D, Antonucci JM and Eanes ED. Amorphous Calcium Phosphate-Based Bioactive Polymeric Composites for Mineralized Tissue Regeneration. J Res Natl Inst Stand Technol 2003; 108:167-182.
69. Yan J, Yang H, Luo T, Hua F and He H. Application of Amorphous Calcium Phosphate Agents in the Prevention and Treatment of Enamel Demineralization. Front Bioeng Biotechnol 2022; 10:853436.
70. Skrtic D and Antonucci JM. Dental composites based on amorphous calcium phosphate-resin composition/physicochemical properties study. J Biomater Appl 2007; 21:375-393.
71. Moszner N and Salz U. New developments of polymeric dental composites. Prog Polym Sci 2001; 26:535-576.
72. Sankarapandian M, Shobha H, Kalachandra S, Mcgrath J and Taylor D. Characterization of some aromatic dimethacrylates for dental composite applications. J Mater Sci Mater Med 1997; 8:465-8.
73. Stansbury JW. Curing dental resins and composites by photopolymerization. J Esthet Restor Dent 2000; 12:300-308.
74. Yoshida K and Greener E. Effects of two amine reducing agents on the degree of conversion and physical properties of an unfilled light-cured resin. Dent Mater 1993; 9:246-251.
75. Yoshida K and Greener E. Effect of photoinitiator on degree of conversion of unfilled light-cured resin. J dent 1994; 22:296-9.
76. Chang JC, Hurst TL, Hart DA and Estey AW. 4-META use in dentistry: a literature review. J Prosthet Dent 2002; 87:216-224.
77. Leung Y and Morris MD. Characterization of the chemical interactions between 4-MET and enamel by Raman spectroscopy. Dent Mater 1995; 11:191-5.
78. Menezes-Silva R, Pereira FV, Santos MH, Soares JA, Soares SMCS and Miranda JLD. Biocompatibility of a New Dental Glass Ionomer Cement with Cellulose Microfibers and Cellulose Nanocrystals. Braz Dent J 2017; 28:172-8.
79. Haydar B, Sarikaya S and Cehreli ZC. Comparison of shear bond strength of three bonding agents with metal and ceramic brackets. Angle Orthod 1999; 69:457-462.
80. Skrtic D, Antonucci JM, Eanes ED and Eidelman N. Dental composites based on hybrid and surface-modified amorphous calcium phosphates. Biomaterials 2004; 25:1141-50.
81. Sabir M, Muhammad N, Siddiqui U, Khan AS, Syed MR, Rahim A, Liaqat S, Shah A. T, Sharif F, Khan MA and Din IU. Effect of nanocrystalline cellulose/silica-based fillers

on mechanical properties of experimental dental adhesive. Polym Bull 2022; 80.

82. Moradian M, Jafarpour D, Saadat M and Tahmasebi F. The effect of bacterial cellulose nanocrystals on the shear bond strength of resin modified glass ionomer cement to dentin. J Clin Exp Dent 2021; 13:e784-8.
83. Antonucci JM, Giuseppetti AA, O'Donnell JNR, Schumacher GE and Skrtic D. Polymerization stress development in dental composites: Effect of cavity design factor. Materials 2009; 2:169-180.
84. Chaudhari PK, Goyal L, Rana SS, Dhingra K and Kshetrimayum N. Nanocomposites and nanoionomers for orthodontic bracket bonding. Applications of Nanocomposite Materials in Dentistry, Elsevier. 2019.
85. Henkin FDS, Macêdo EDODD, Santos KDS, Schwarzbach M, Samuel SMW and Mundstock KS. In vitro analysis of shear bond strength and adhesive remnant index of different metal brackets. Dental Press J Orthod 2016; 21:67-73.
86. Leão Filho JCB, Braz AKS, Araujo RE, Tanaka OM and Pithon MM. Enamel quality after debonding: evaluation by optical coherence tomography. Braz Dent J 2015; 26:384-9.
87. Faria-Júnior ÉM, Guiraldo RD, Berger SB, Correr AB, Correr-Sobrinho L, Contreras EFR and Lopes MB. In-vivo evaluation of the surface roughness and morphology of enamel after bracket removal and polishing by different techniques. Am J Orthod Dentofacial Orthop 2015; 147:324-9.
88. Santos LK, Rocha RH, Pereira Barroso AC, Otoni RP, Carvalho de Oliveira Santos C and Fonseca-Silva T. Comparative analysis of adhesive remnant index of orthodontic adhesive systems. South Eur J Orthod Dentofac Res 2021; 8:26-30.
89. Sharma S, Tandon P, Nagar A, Singh GP, Singh A and Chugh VK. A comparison of shear bond strength of orthodontic brackets bonded with four different orthodontic adhesives. J Orthod Sci 2014; 3:29-33.